Vibration Characteristics of Hexagonal Radial Rib and Hoop Platforms

W. Keith Belvin*
NASA Langley Research Center, Hampton, Virginia

The modes of vibration of planar radial rib and hoop hexagonal platforms have been characterized by both experiment and analysis. The sensitivity of mode shapes and frequencies to cable stiffness and preload is presented. Primary vibration modes of the radial rib platform involve beam bending. Vibration modes of the hoop platform exhibit beam bending, frame bending, and torsion. Linear finite element analysis correlates well with experimental data. Threshold stiffness values have been identified above which changes in cable stiffness do not affect the first few platform modes. Above the threshold levels of cable stiffness, nodes are formed at the cable to beam attachment points, which precludes cable slackening due to vibrations in these modes.

Nomenclature

A_c = cable cross-sectional area
E = Young's modulus of beam material
E_c = Young's modulus of cable material
G = shear modulus of beam material
I = beam area moment of inertia
J = beam torsional constant
$\bar{K}$ = stiffness parameter, Eq. (3)
L = cable and beam element length
M = beam mass, kg
M_c = cable mass, kg
$\bar{M}$ = mass parameter, M_c/M, Eq. (4)
n = integer representing nth cable mode, $n = 1, 2, 3, \ldots$
NS = number of sides, NS = 6 for hexagonal geometry
P = compressive load in the beams, equal in magnitude to T for hexagonal geometry
P_e = Euler buckling load
R = radius of platform
T = cable tension
ω = platform natural frequency, rad/s
ω_{ss} = fundamental bending frequency of a simply supported beam, rad/s
$\bar{\omega}$ = frequency parameter, ω/ω_{ss}, Eq. (1)

Introduction

TO establish large structural configurations in space for communications and solar power generation, numerous antenna and platform structural concepts have been suggested. Examples of proposed structural concepts are the radial rib antenna[1] and the hoop solar power system[2] shown in Fig. 1. The radial rib antenna consists of parabolically curved beams attached radially to a central hub. The antenna surface is formed by attaching a reflecting membrane mesh to the ribs. The solar power system consists of a hexagonal hoop platform which supports a membrane covered with photovoltaic cells. A common characteristic of these structures is the use of either radial rib or hoop platforms to provide global stiffness and to carry compressive reaction loads produced by pretensioned cables and membranes. In addition to the global use of radial rib and hoop platforms, structures consisting of an assemblage of radial rib and/or hoop hexagonal facets also have been proposed.[3]

Vibration analysis of large space structures is required to determine the magnitude and duration of vibrations due to maneuvers and other disturbances. The large size of the analytical models often makes parameter studies economically infeasible. Thus, it is often desirable to study simpler structures which have similar characteristics, to obtain a fundamental understanding of the vibration behavior. With numerous applications of the radial rib and hoop concepts proposed, the need exists to identify general vibration characteristics which may occur in any radial rib or hoop structure. This may be accomplished by investigating generic radial rib and hoop structures such as the cable-stiffened platforms shown in Fig. 2. However, previous studies[4,5] of cable-stiffened structures have shown nonlinear vibrations at relatively small deflections. Experimental data from Ref. 4 also indicates significant reductions in static stability due to small dynamic excitations. Thus, to ensure the suitability of linear analysis to study such structures, an accompanying experimental study is desirable.

This paper presents the results of an analytical and experimental investigation of the general vibration characteristics of hexagonal radial rib and hoop planar platforms. The in-plane and out-of-plane frequencies and mode shapes of each model were measured with and without cables. Cable tension was varied during the test program to evaluate preload effects. Both experimental models were also evaluated using linear finite element analysis and the vibration characteristics

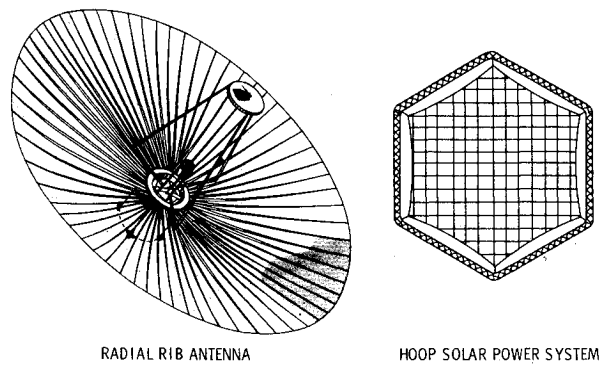

Fig. 1 Proposed radial rib and hoop structures.

Presented as Paper 83-0822 at the AIAA/ASME/ASCE/AHS 24th Structures, Structural Dynamics and Materials Conference, Lake Tahoe, Nev., May 2-4, 1983; submitted June 3, 1983; revision received July 9, 1984. This paper is declared a work of the U.S. Government and therefore is in the public domain.

*Aerospace Engineer, Structures and Dynamics Division, Structural Dynamics Branch. Member AIAA.

from analysis and test are compared. Analytical models are also used to evaluate the sensitivity of mode shapes and frequencies to cable stiffness and tension levels. In addition, physical interpretation of the modes is presented to enhance understanding of more complex platform vibrations.

Models

Experimental

Tests of the hexagonal platform were conducted to verify analytical results and to reveal unanticipated vibration behavior. The experimental models, shown in Fig. 2, were constructed from rectangular aluminum beams 6.35 mm thick and 50.8 mm wide. The beams were oriented such that the minimum bending stiffness was in-plane. Turnbuckles and 1.59-mm-diameter steel cables were used to preload and stiffen the platforms. Each beam and cable element length L is 1.0 m. All beam-to-beam joints were welded in the radial rib model, whereas the hoop model joints were rigidly bolted.

Vibration tests were performed to ascertain natural frequencies and mode shapes, with and without cables. The platforms were supported from low-stiffness cables (horizontally for in-plane modes and vertically for out-of-plane modes) to approximate free-free boundary conditions. Excitation was provided by one or both of the electrodynamic shakers located schematically in Fig. 3. Symmetric and antisymmetric modes could be excited separately by operating the shakers in-phase or 180 deg out-of-phase, respectively. The models were instrumented with accelerometers to measure the response due to a nominal 0.5 N sinusoidal force. In-plane modes were measured by 24 accelerometers, located as shown in Fig. 3. Out-of-plane modes were excited and measured similarly to the in-plane modes, with shakers and accelerometers oriented out-of-plane. Only 18 accelerometers were used.

To determine the effect of cable preload, tests at various tension levels were performed. Back-to-back strain gages were used to measure initial axial strain in the beams due to cable preload. Since each beam and cable element had equal and opposite preload, the cable tension was computed from the strain in the beams.

Analytical

Two NASTRAN[6] (registered trademark of NASA) finite-element models were used to predict the modes of the hexagonal platforms: a detailed model consisting of 10 BAR elements in each beam member and one ROD element for each cable member, and a simplified model with only four BAR elements in each beam member. The detailed model was used to check convergence of the simpler model and to produce mode shape plots. The simplified model was used to make cable stiffness and tension parameter studies. The axial cable stiffness and the cable tension level were varied to determine frequency and mode shape sensitivity. NASTRAN Rigid Format 13 was used to include the differential stiffness effects. No dynamic reduction was employed on either model.

Analysis models used for experimental correlation contained nonstructural mass representing the effective mass of accelerometers, turnbuckles, and shakers. Other analytical results do not include this additional mass. Boundary conditions on all analyses are free-free to approximate the experimental cable supports.

Dimensionless Parameters

Several dimensionless parameters have been used to present the results. This enables results from this study to be extended to any size of geometrically similar structure. The natural frequency ω is nondimensionalized to the frequency of a simply-supported beam of length L, such that

$$\bar{\omega}^2 = \omega^2/\omega_{ss}^2 = \omega^2 L^3 M/\pi^4 EI \tag{1}$$

For out-of-plane modes the out-of-plane bending stiffness is used to compute ω_{ss}. Similarly, for in-plane modes in-plane bending stiffness is used. For the experimental models, the values of ω_{ss} are $\omega_{ss}=740.3$ rad/s, out-of-plane, and $\omega_{ss}=92.54$ rad/s in-plane. The cable preload, P, is nondimensionalized to the Euler buckling load of a beam element

$$\bar{P}=P/P_e=PL^2/\pi^2 EI \tag{2}$$

The Euler load of the experimental models is computed to be $P_e=48.61$ kN out-of-plane, and $P_e=759.6$ N in-plane.

When stiffening cables are used, the chosen properties and sizes of the experimental model result in dimensionless stiffness and mass parameters of

$$\bar{K}=E_c A_c L^2/EI=2200 \tag{3}$$

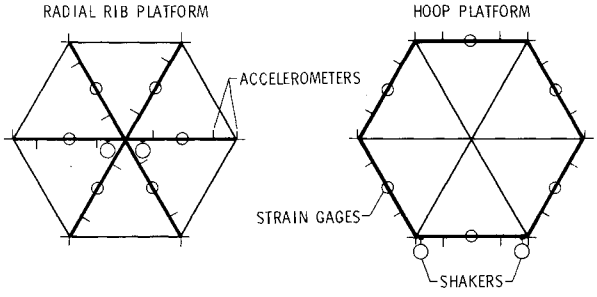

Fig. 3 Experimental in-plane instrumentation locations.

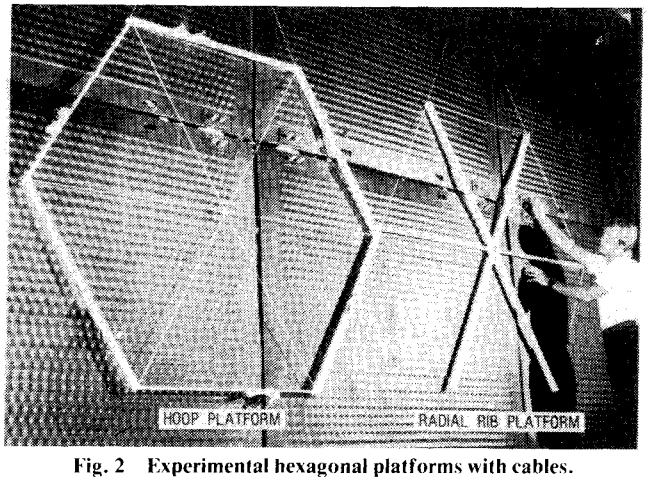

Fig. 2 Experimental hexagonal platforms with cables.

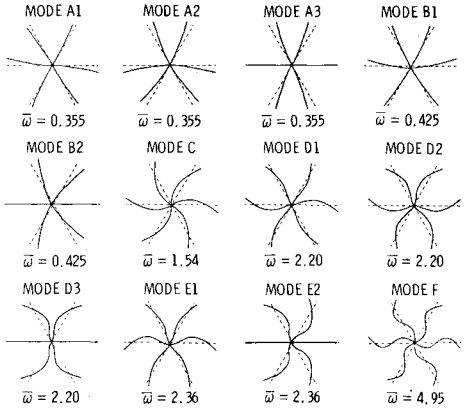

Fig. 4 Analytical in-plane mode shapes of the radial rib platform without cables.

and

$$\bar{M} = M_c/M = 0.0176 \quad (4)$$

The experimental stiffness value, $\bar{K} = 2200$, was obtained from axial cable stiffness measurements and nondimensionalized by the in-plane bending stiffness.

Results and Discussion

Results of vibration analyses and tests are presented for the radial rib and hoop platforms. Four test setups have been studied for each platform: in-plane vibrations with and without cables and out-of-plane vibrations with and without cables. Tension level effects on in-plane vibration frequencies are presented both from test and analysis. The chosen experimental model dimensions produced in-plane buckling before out-of-plane buckling occurred, hence out-of-plane tension level effects were studied only analytically. The effect of cable stiffness was studied analytically for $0 \le \bar{K} \le 2200$. Analysis and test results are compared at the upper and lower limits of this range.

Modes have been identified by a letter followed by a number whenever more than one mode shape occurs at the same frequency. Unique letters are assigned to the four cases as follows:

Case	Mode identification
Radial rib platform, in-plane	A-F
Radial rib platform, out-of-plane	G-K
Hoop platform, in-plane	L-R
Hoop platform, out-of-plane	S-Y

For each case, all modes up to a cutoff frequency of $\bar{\omega} = 4.0$ are presented. This cutoff frequency represents the second simply supported mode of a beam of length L.

Radial rib platform results are presented first followed by hoop platform results.

In-Plane Vibrations of Radial Rib Model

Radial Rib Model Without Cables

The first 12 in-plane analytical modes shape of the radial rib platform are shown in Fig. 4. Parameter values without cables are $\bar{K} = \bar{M} = \bar{P} = 0$. Several mode shapes may occur at the fundamental frequency $\bar{\omega} = 0.355$. These mode shapes are combinations of the individual members first cantilever mode. The mode shapes at $\bar{\omega} = 0.425$ are similar to cantilever beam modes, except that a net translation of the platform is required for momentum balance. To produce platform translation or rotation, additional energy is required which results in a higher frequency. Mode C is the second pinned-free mode of each beam. Note that since all six beams are in phase, no moment exists at the hub. The frequency predicted by finite element analysis is one percent lower than exact analysis predicts. The lower frequency is probably due to the use of a lumped mass matrix in the finite element analysis. Both modes D and E are composed of members vibrating in the second cantilever bending modes, with the higher frequency involving platform translation. The final mode shape is the third pinned-free beam bending.

Experimental and analytical frequency correlation is shown in Table 1. Note that the analytical frequencies differ from those of Fig. 4 due to the inclusion of instrumentation mass. The experimental frequencies agree very closely with analysis. Though several mode shapes often are predicted at one frequency by analysis, one dominant mode shape usually occurred experimentally. Only modes A2, B1, C, D1, D2, E1, and F were observed.

Radial Rib Model With Cables

Figure 5 shows the first seven in-plane analytical mode shapes for the cable stiffened platform. Mode shape C is torsional about the hub as described in the previous section. The second natural frequency, $\bar{\omega} = 1.55$, has three possible mode shapes which are characterized predominantly by clamped-pinned beam vibration. Experimentally mode A1 was measured at this frequency. Modes A2 and A3 were not detected by conventional sine-sweep modal tests. Table 1 shows that the largest percent difference in frequency between analysis and test, 5.2%, was detected for mode A1. At $\bar{\omega} = 1.95$, clamped-pinned behavior is predominant, but for inertial balance the entire platform must translate. The final mode shape shown in Fig. 5, mode F, represents the third pinned-free mode of each beam.

Test and analysis results for various values of the load parameter $\bar{P}$ are shown in Fig. 6. Good agreement is obtained between analysis and experiment for modes A, B, and C. The square of the frequency decreases linearly as the preload is increased. This indicates that the mode shapes do not change. Experimental data above $\bar{P} = 0.67$ was not obtained due to large growth in the lateral eccentricity of the beam members.

Table 1 In-plane radial rib platform frequencies, $\bar{\omega}$

Mode	Without cables		With cables $\bar{P} = 0.01$	
	Analysis[a]	Experiment	Analysis[a]	Experiment
A1	0.354	–	1.53	1.45
A2	0.354	0.345	1.53	–
A3	0.354	–	1.53	–
B1	0.422	0.400	1.91	1.88
B2	0.422	–	1.91	–
C	1.42	1.39	1.34	1.30
D1	2.13	2.05	[b]	[b]
D2	2.13	2.14	[b]	[b]
D3	2.13	–	[b]	[b]
E1	2.34	2.21	[b]	[b]
E2	2.34	–	[b]	[b]
F	4.66	4.53	4.60	4.38

[a] Includes instrumentation mass. [b] Above cutoff frequency.

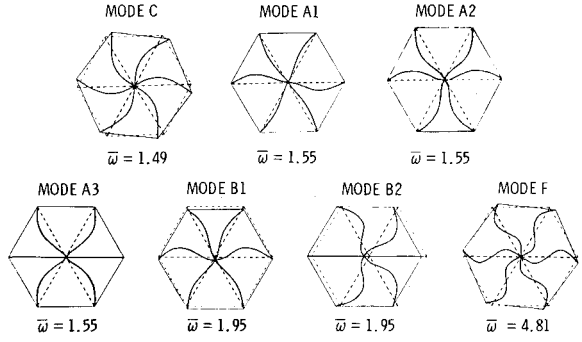

Fig 5 Analytical in-plane mode shapes of the radial rib platform with cables, $\bar{K} = 2200$, $\bar{M} = 0.01$, $\bar{P} = 0.01$.

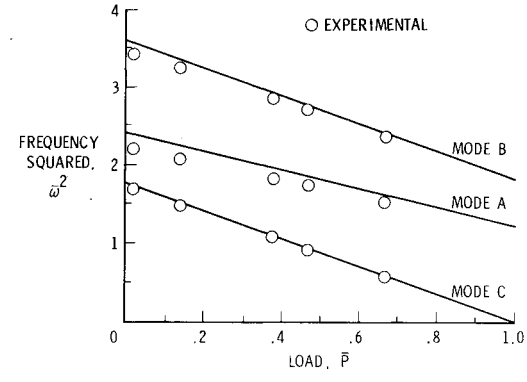

Fig. 6 Radial rib platform in-plane frequency variation with load, $\bar{K} = 2200$, $\bar{M} = 0.0176$.

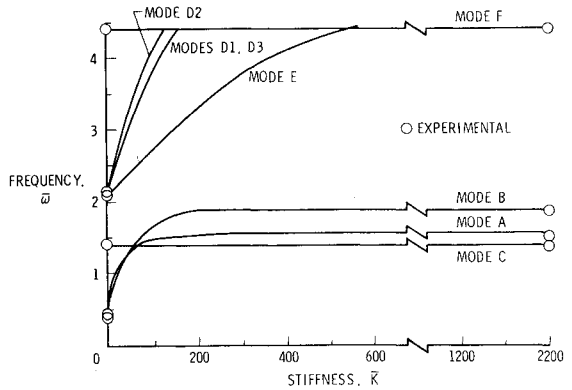

Fig. 7 Radial rib platform in-plane frequency variation with stiffness, $\bar{M}=0.01$, $\bar{P}=0.01$.

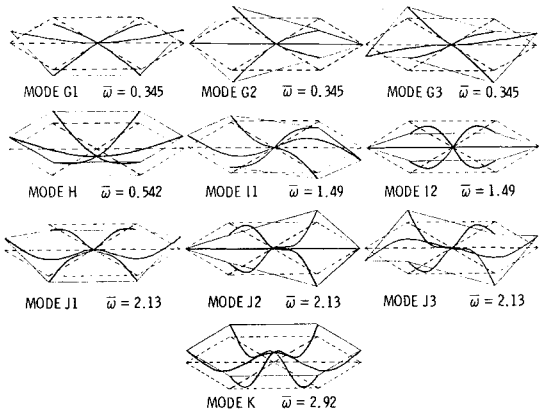

Fig. 8 Analytical out-of-plane mode shapes of the radial rib platform with cables, $\bar{K}=2200$, $\bar{M}=0.01$, $\bar{P}=0.002$.

To assess the effects of cable stiffness, the stiffness parameter $\bar{K}$ was analytically varied from a value of 0 to 2200. For $\bar{K}=0$, the model represents a radial rib platform without cables. Frequency variation with cable stiffness is shown in Fig. 7. As the stiffness is increased, the first two natural frequencies, modes A and B, approach the frequencies of the model with cables, and the mode shapes A and B of Fig. 4 transform from clamped-free to the clamped-pinned mode shapes of Fig. 5. Modes C and F are insensitive to the stiffness parameter since no relative displacement occurs between the ends of adjacent beams.

Results shown in Fig. 7 indicate a threshold value of the stiffness parameter above which modes A, B, C, and F become insensitive to $\bar{K}$. This is important because nonlinear vibrations due to cable slackening in these modes can be avoided by designing the stiffness parameter to exceed this threshold value of $\bar{K}\geq 600$. The usual method to prevent cable slackening is to pretension the cables sufficiently such that cable loads remain tensile during vibration. This method may require high levels of pretension which reduces the frequencies and stability of the structure as previously shown. By designing above the threshold stiffness value, nodes are formed at the cable attachment points and the cable load remains constant during vibration for the first four modes of the radial rib model.

Out-of-Plane Vibrations of the Radial Rib Model

Correlation of experiment and analysis for the radial rib out-of-plane frequencies is presented in Table 2. Again, very good agreement is shown. Since the cables lie in the plane of the platform, they do not contribute out-of-plane stiffness for linear deflections. However, the cable tension does contribute

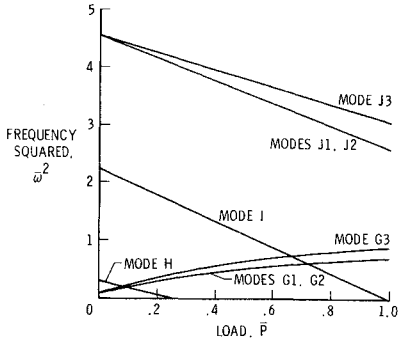

Fig. 9 Radial rib platform out-of-plane frequency variation with load, $\bar{K}=2200$, $\bar{M}=0.01$.

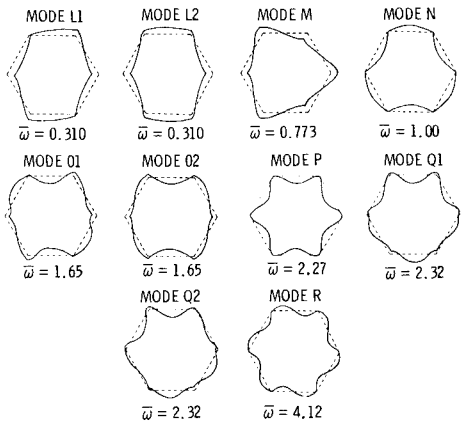

Fig. 10 Analytical in-plane mode shapes of the hoop platform without cables.

Table 2 Out-of-plane radial rib platform frequencies, $\bar{\omega}$

Mode	Without cables		With cables $\bar{P}=0.002$	
	Analysis[a]	Experiment	Analysis[a]	Experiment
G1	0.355	0.343	0.345	0.327
G2	0.355	–	0.345	–
G3	0.355	0.349	0.345	0.344
H	0.562	0.557	0.542	0.541
I1	1.54	1.43	1.49	1.37
I2	1.54	1.46	1.49	1.41
J1	2.20	2.19	2.13	2.18
J2	2.20	–	2.13	–
J3	2.20	2.20	2.13	2.20
K	3.01	3.00	2.92	2.96

[a] Includes instrumentation mass.

out-of-plane stiffness. Thus, at low tension levels, there exist only small frequency differences in the out-of-plane modes with and without cables. These differences can be attributed almost entirely to the additional cable mass at the tension level shown in Table 2, $\bar{P}=0.002$. The analytical mode shapes and frequencies are shown in Fig. 8.

The first three mode shapes, at $\bar{\omega}=0.345$, are first cantilever bending modes. Mode H is the first free-free bending of a beam of length $2L$. Mode I is the second pinned-free mode of each beam. The next three modes, $\bar{\omega}=2.13$, are similar to beam clamped-pinned modes with platform translation. The last mode, mode K, is predominantly clamped-pinned beam vibration with all six beams in phase. This requires an even higher frequency to maintain inertial balance $\bar{\omega}=2.92$.

Analytical frequency variation with preload of the radial rib out-of-plane modes is shown in Fig 9. Preload has both a

Table 3 In-plane hoop platform frequencies, $\bar{\omega}$

Mode	Without cables		With cables $\bar{P}=0.01$	
	Analysis[a]	Experiment	Analysis[a]	Experiment
L1	0.311	–	1.24	–
L2	0.311	0.293	1.24	1.22
M	0.773	0.757	[b]	[b]
N	1.00	0.995	0.993	0.991
O1	1.64	–	[b]	[b]
O2	1.64	1.61	[b]	[b]
P	2.26	2.25	2.24	2.22
Q1	2.29	–	2.27	2.26
Q2	2.29	2.28	2.27	–
R	4.05	4.00	3.97	3.93

[a] Includes instrumentation mass. [b] Above cutoff frequency.

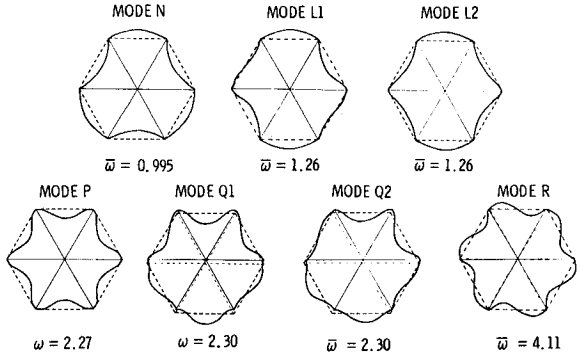

Fig. 11 Analytical in-plane mode shapes of the hoop platform with cables, $\bar{K}=2200$, $\bar{M}=0.01$, $\bar{P}=0.01$.

hardening and softening effect. Mode G increases in frequency as the preload is increased. This increase is due to the increase in out-of-plane stiffness resulting from cable tension at the beam ends. The remaining modes decrease in frequency due to increasing beam compression. Mode H approaches zero frequency at the preload $\bar{P}=0.25$. This is the Euler load of a beam of length $2L$. Mode I approaches zero frequency at the Euler buckling load. Figure 9 should be used only for frequency trends, since mode shapes will couple as two symmetric or antisymmetric modes approach the same frequency. At $\bar{P}=0.09$, an optimal tension level is indicated at which the highest out-of-plane fundamental frequency occurs for the radial rib platform.

In-Plane Vibrations of the Hoop Model

Hoop Model Without Cables

Results similar to those presented for the radial rib platform have been obtained for the hoop platform. As seen in Fig. 10, the first 10 analytical mode shapes for in-plane vibrations exhibit both frame and beam vibration characteristics. Modes L and M exhibit global frame bending. The next mode, mode N, is the first simply supported beam mode. Mode O exhibits both beam and frame bending at $\bar{\omega}=1.65$. Modes P and Q are predominantly clamped-clamped beam vibration with mode Q also involving platform translation. The mode shape at $\bar{\omega}=4.12$, mode R, is second simply supported beam bending with platform rotation. Test and analysis frequency results are shown in Table 3. The dominant shapes observed during tests are modes L2, M, N, O2, P, Q2, and R. The remaining mode shapes were not observed in the experimental model.

Hoop Model With Cables

The first seven analytical in-plane mode shapes are shown in Fig. 11. The fundamental mode, first simply supported beam bending, occurs at a frequency of $\bar{\omega}=0.995$. Comparatively, the radial rib platform in-plane fundamental frequency is 50% higher than the hoop frequency. The next two modes exhibit clamped pinned beam vibrations. Clamped-clamped vibration is present in the next three modes, with mode Q possessing a higher frequency than mode P due to additional platform translation. The final mode shown in Fig. 11 is the second simply-supported beam bending. Table 3 shows the maximum frequency difference between analysis and test to be only 1.6%.

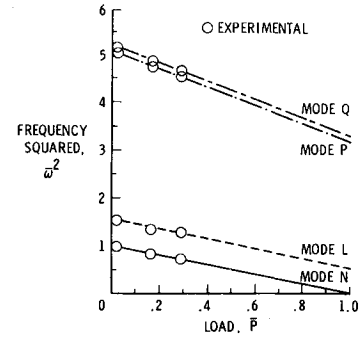

Fig. 12 Hoop platform in-plane frequency variation with load, $\bar{K}=2200$, $\bar{M}=0.0176$.

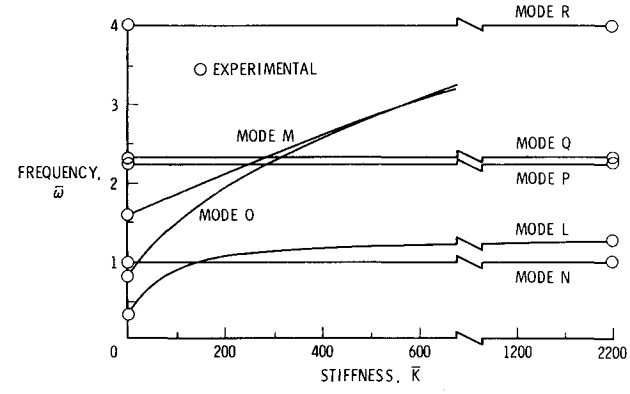

Fig. 13 Hoop platform frequency variation with stiffness, $\bar{M}=0.01$, $\bar{P}=0.01$.

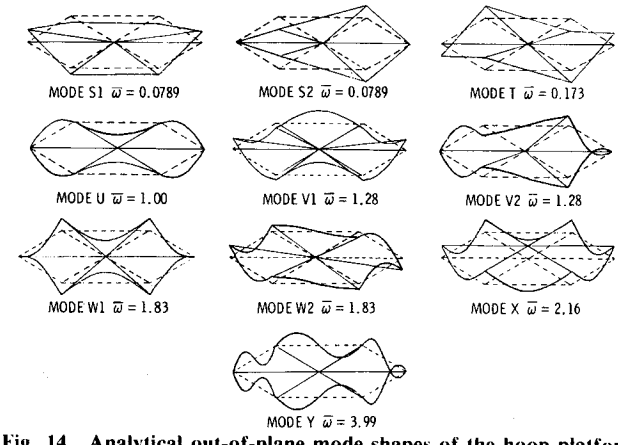

Fig. 14 Analytical out-of-plane mode shapes of the hoop platform with cables, $\bar{K}=2200$, $\bar{M}=0.01$, $\bar{P}=0.002$.

Variation of frequency with preload is shown in Fig. 12. The reduction in the square of the frequency is linear with preload as expected. No experimental data was obtained above $\bar{P}=0.29$ since very good correlation had been established. Cable stiffness effects are shown in Fig. 13. Experimental data is shown at the upper and lower limits for correlation with analysis. Mode data marked L is strongly dependent on cable stiffness. This mode changes shape, as can be seen in comparing modes L1 and L2 in Figs. 10 and 11, and becomes insensitive to cable stiffness at $\bar{K}\geq 600$. Although not

shown on the figure, modes M and O increase in frequency with increasing cable stiffness, even at $\bar{K}=2200$. These modes become higher in frequency than do the first seven modes for $\bar{K}\geq 1000$. The remaining modes are insensitive to cable stiffness, and possess the same mode shapes and frequencies with and without cables for low values of preload. Again, cable slackening may be avoided in the first five modes of the hoop model by designing the stiffness parameter such that $\bar{K}\geq 1000$.

Out-of-Plane Vibrations of the Hoop Model

As mentioned earlier, the cable stiffness does not affect out-of-plane vibrations based on linear analysis; however, cable preload and mass do affect the frequency of vibration. For low values of the preload and mass parameters, only small differences in frequency exist for the platform with and without cables. Table 4 shows experimental and analytical results for the unstiffened and stiffened hoop for $\bar{M}=0.0176$ and $\bar{P}=0.002$. Correlation between analysis and test is good.

Analytical out-of-plane mode shapes with cables are shown in Fig. 14. Modes S and T are predominantly frame torsion modes and are strongly dependent on the torsional beam stiffness, GJ. Mode U is first simply-supported beam bending. Modes V and W possess both frame torsion and beam bending characteristics. Modes X and Y are the clamped-clamped and second simply-supported beam modes, respectively.

Preload effects on the hoop out-of-plane modes are shown in Fig. 15. The frequency of modes S and T approach zero at very low values of the preload parameter, $\bar{P}=0.0287$ and 0.0696, respectively. The frequency of mode U approaches zero at $\bar{P}=1.0$ as expected.

Some of the out-of-plane hoop modes involve torsion of the platform; therefore, the frequency is dependent on a torsional stiffness parameter, GJ/EI. The rectangular cross section chosen for the experimental models produced a low value of the parameter, $GJ/EI=0.023$. This results in the out-of-plane fundamental frequency of the hoop model to be lower than the radial rib model. Figure 16 shows the effect of torsional stiffness on the frequency of the first eight modes. As GJ/EI increases, the frequencies of those modes involving torsion increase. Experimental data points show the value of GJ/EI chosen for the test model. If circular cross section aluminum beams had been chosen, the torsional stiffness parameter would be $GJ/EI=0.74$, as indicated on Fig. 16. Higher values of the torsional stiffness will require tailoring of orthotropic materials or special construction such as lattice beams. Out-of-plane modes of hoop and radial rib structures would be constrained by additional cable stiffness in a three-dimensional structure such as an antenna. Thus, the out-of-plane results are most applicable to planar structures such as the solar power system.[2]

Comparison of Fundamental In-Plane Frequency

Comparison of the hexagonal radial rib and hoop platform vibrations indicates the radial rib concept produced a higher fundamental in-plane frequency than the hoop concept. To evaluate other polygonal shapes, analyses were made for structures with an even number of sides, NS, from four to 20. Figure 17 shows the predicted change in fundamental in-plane frequency as the number of sides is varied. In this figure, the cable mass per unit length is one percent of the beam mass per length. The radius of each polygon is R and the modified stiffness parameter

$$E_c A_c R^2/EI = 2200$$

The fundamental in-plane mode of the hexagonal cable stiffened radial rib platform does not change considerably as the number of beam elements is increased. The mode shape is second pinned-free beam bending. As the number of sides is increased, the hoop platform approaches a ring and the cables act as an in-plane elastic foundation. Modes of this structure will exhibit ring bending in-plane. Figure 17 indicates that for low-order polygonal structures the radial rib concept produces the highest in-plane fundamental frequency. For octagonal or higher-order polygonal structures, the hoop concept produces the highest frequency.

Table 4 Out-of-plane hoop platform frequencies, $\bar{\omega}$

Mode	Without cables		With cables $\bar{P}=0.002$	
	Analysis[a]	Experiment	Analysis[a]	Experiment
S1	0.0825	0.0839	0.0754	0.0756
S2	0.0825	–	0.0754	–
T	0.172	0.168	0.165	0.163
U	1.00	1.00	1.00	1.00
V1	1.25	1.27	1.24	1.27
V2	1.25	–	1.24	–
W	1.78	1.78	1.78	1.76
X	2.12	2.04	2.10	2.03
Y	4.00	3.96	4.00	3.95

[a] Includes instrumentation mass.

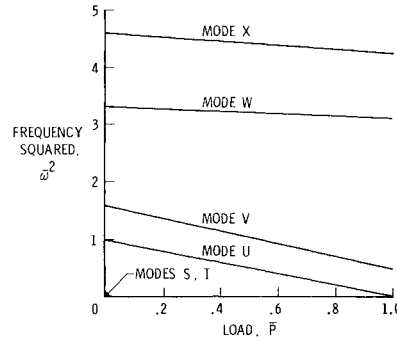

Fig. 15 Hoop platform frequency variation with load, $\bar{K}=2200$, $\bar{M}=0.01$.

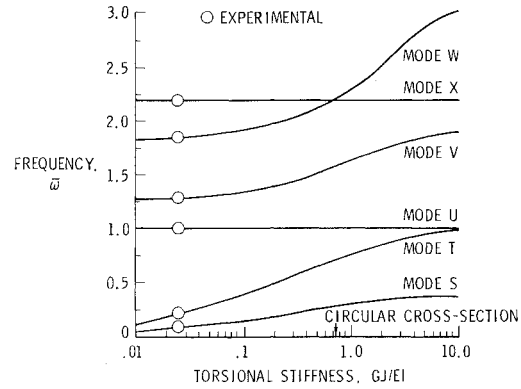

Fig. 16 Hoop platform out-of-plane frequency variation with stiffness, $\bar{M}=0.01$, $\bar{P}=0.002$.

Cable Modes

The radial rib and hoop modes presented thus far have neglected distributed cable inertial effects. It has been shown previously[5] that the distributed mass of the cables usually can be lumped at the ends when the ratio of cable mass to the effective member mass to which it connects is small. When modes dominated by cable deflections are of interest, the simple taut string frequency equation yields good results

$$\omega_n^2 = n^2\pi^2 T/LM_c \qquad (5)$$

To determine the fundamental in-plane cable mode, ω_1, of the hoop and radial rib platforms, Eq. (5) may be used. The

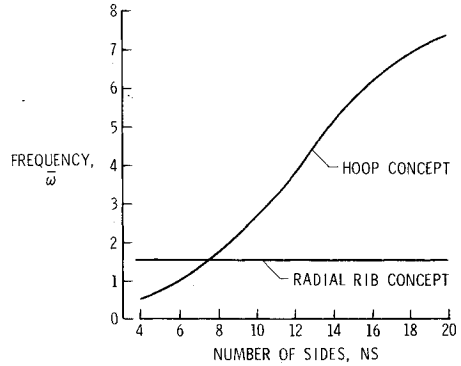

Fig. 17 Change in fundamental in-plane frequency with the number of sides in the radial rib and hoop concepts.

fundamental out-of-plane radial rib cable mode can also be determined from Eq. (5). The fundamental out-of-plane hoop platform cable mode has an effective length of 2L since the cables connect to each other in the center. Thus, for the hoop cable mode

$$\omega_1^2 = \pi^2 T/4LM_c \tag{6}$$

Equations (5) and (6) as appropriate should be used in conjunction with Figs. 6, 9, 11, and 15 to choose the optimum preload value for maximum fundamental frequency.

Concluding Remarks

An experimental and analytical investigation of the vibration characteristics of radial rib and hoop hexagonal platforms has been performed. Good test and analysis correlation shows no need for unusual modeling techniques for linear vibrations.

Inceasing cable tension reduces the frequency of all modes dominated by beam deflections except for the first three out-of-plane modes of the radial rib platform. Cable modes increase in frequency with increasing tension. As the cable stiffness is inceased from zero, the in-plane modes change shape and increase in frequency. A threshold value exists above which the first few modes become insensitve to further changes in stiffness. By designing above the threshold cable stiffness value, the cable loads remain constant during vibration for the first few modes of both platforms. This constant cable load precludes nonlinear vibrations due to cable slackening in these modes.

Primary vibration modes of the radial rib platform involve beam bending. Some of these modes are easily identified and the frequency often can be predicted on the basis of a single vibrating beam. However, other modes exhibit platform rotation or translation to maintain inertial force balance and the frequency cannot be predicted by considering a single vibrating beam. Vibration modes of the hoop platform possess beam bending and frame bending and torsion. These modes require frame analysis to predict mode shapes and frequencies. Results indicate that for low-order polygonal structures, the radial rib concept produces the highest fundamental in-plane frequency. For octagonal or higher-ordered polygonal structures, the hoop concept may achieve a higher fundamental frequency than the radial rib concept by proper selection of cable stiffness.

References

[1] Woods, A.A. Jr., "Offset Wrap Rib Antenna Concept Development," NASA CP 2168, Vol. 1, Nov. 1980.

[2] Greenberg, H.S., "Satellite Power Systems SPS-LSST Systems Analysis and Integration Task for SPS Flight Test Article," NASA CR-3375, Feb. 1981.

[3] Agrawal, P.K., Anderson, M.S., and Card, M.F., "Preliminary Design of Large Reflectors with Flat Facets," *IEEE Transactions on Antennas and Propogation,* Vol. AP-29, No. 4, July 1981, pp. 688-694.

[4] Belvin, W.K., "Analytical and Experimental Vibration and Buckling Characteristics of a Pretensioned Stayed Column," AIAA Paper 82-0775, May 1982.

[5] Housner, J.M. and Belvin, W.K., "On the Analytical Modeling of the Nonlinear Vibrations of Pretensioned Space Structures," *Computers and Structures,* Vol. 16, No. 1-4, 1983, pp. 339-352.

[6] NASTRAN Users Manual (Level 17.5), NASA SP-222 (05), 1978.